Austenite Formation during Intercritical Annealing

J. HUANG, W.J. POOLE, and M. MILITZER

A systematic experimental study has been conducted on ferrite recrystallization and intercritical austenite formation for two low-carbon steels with chemical compositions typically used for dual-phase and transformation-induced plasticity (TRIP) steels. Different initial heating rates, holding temperatures, and times were applied to the materials to examine the ferrite recrystallization and austenite formation kinetics. An Avrami model was developed to describe the isothermal ferrite recrystallization behavior and was applied successfully to the nonisothermal conditions. It was found that the initial heating rate affects the isothermal austenite formation kinetics for both the hot-rolled and cold-rolled materials albeit the effect is more pronounced for the cold-rolled material. This can be attributed to the interaction between the ferrite recrystallization and austenite formation processes. Furthermore, it was found that the distribution of austenite phase is also affected by the ferrite recrystallization process. When ferrite recrystallization is completed before the austenite formation (*i.e.*, under sufficiently slow heating rate conditions), austenite is to a large extent randomly distributed in the ferrite matrix. On the other hand, incomplete recrystallization of ferrite due to higher heating rates leads to the formation of banded austenite grains. It is proposed that this observation is characteristic of simultaneous recrystallization and austenite formation where moving ferrite grain boundaries do not provide suitable sites for austenite nucleation.

I. INTRODUCTION

THERE is currently a large interest in producing steels with superior mechanical behavior as, *e.g.*, provided by dual-phase (ferrite/martensite) and transformation-induced plasticity (TRIP) steels. To generate the required microstructures, a processing route can be used, which involves cold rolling of ferrite/pearlite microstructures followed by intercritical annealing on a continuous annealing line, usually a hot dip galvanizing line. This processing route can be used to produce multiphase steels such as dual-phase (ferrite/martensite) and TRIP steels; the latter have a substantial fraction of retained austenite (5 to 20 pct). Although a general understanding of these materials has been developed, a number of fundamental issues remain to be solved. Furthermore, experience has shown that these steels are considerably more sensitive to production variations compared to conventional steels. A careful control of processing conditions and the identification of critical processing steps is crucial to the success of these products. The challenge, therefore, is to develop industrially relevant processing routes that will lead to the desired properties with a minimum of variation.

The processing routes for cold-rolled and annealed dual-phase and TRIP steels involve reheating the steel into the intercritical region, where an austenite/ferrite mixture is formed. For dual-phase steels, cooling to room temperature produces a microstructure consisting of ferrite and martensite. The cooling path and composition of these steels must be carefully optimized to minimize transformation back to ferrite or the pearlite and bainite reactions. This is usually facilitated by alloy additions such as Mn, Mo, or Cr. In the case of TRIP steels, cooling followed by holding at an intermediate temperature in the bainite transformation range is required to carefully control the decomposition of austenite into bainite and martensite, with some austenite retained in the final microstructure. Again, alloying additions play a critical role, in this case, usually a combination of Mn, Si, and more recently Al. The addition of Si or Al is required to minimize carbide precipitation, thereby enabling austenite retention at room temperature. The mechanical properties of the dual-phase and TRIP steels are primarily dependent on the volume fraction, carbon concentration, and distribution of the final transformation products,[1,2] which inherit the composition and distribution of the parent austenite phase. Therefore, the austenite condition at the intercritical temperature is important for the evolution of the final microstructure of the steel and consequently its mechanical properties.

The formation of austenite has been widely investigated over the last century albeit not as extensively as austenite decomposition. What appears to be the first account that austenite forms as a nucleation and growth process upon heating can be traced to Arnold and McWilliams.[3] Roberts and Mehl[4] confirmed the nucleation and growth nature of the process by discussing in detail the rate of austenite formation from ferrite-cementite aggregates. A substantial body of work was published in the 1980s in conjunction with extensive research on dual-phase steels.[5–18] For example, Speich *et al.*[6] investigated austenite formation in 1.5 wt pct Mn steels containing 0.06 to 0.20 wt pct carbon with ferrite-pearlite microstructures. They concluded that austenite formation can be separated into three stages: (1) very rapid growth of austenite into pearlite until complete pearlite dissolution, (2) slower growth of austenite into ferrite primarily controlled by carbon diffusion in austenite, and (3) very slow equilibration of austenite and ferrite controlled by manganese diffusion in austenite. Garcia and DeArdo[5] conducted similar studies on 1.5 wt pct Mn steels but included also primarily ferritic steels with carbon contents as low as 0.01 wt pct. In general, the nucleation of austenite is associated with cementite precipitates and, thus, potential nucleation sites are ferrite/pearlite interfaces and cementite particles at ferrite grain boundaries.[19] These generally accepted mechanisms of austenite formation

J. HUANG, Graduate Student, W.J. POOLE, Associate Professor, and M. MILITZER, Associate Professor, are with the Department of Materials Engineering, The University of British Columbia, Vancouver, BC, Canada V6T 1Z4. Contact e-mail: hjin@interchange.ubc.ca

Manuscript submitted March 24, 2004.

are based primarily on isothermal studies on hot-rolled or fully annealed steels. Little information is available on the effect of cold rolling and heating rate on the austenite formation in the intercritical temperature range.[9,14,20,21] Petrov *et al.*[22] have recently suggested that in a C-Mn-Si TRIP steel, austenite formation occurs in nonrecrystallized ferrite during ultrafast heating (>1000 °C/s) leading to a refined microstructure as compared to more conventional heating rates (<50 °C/s). The substantial role of the degree of ferrite recrystallization is consistent with an earlier study by Yang *et al.*[20] who observed a strong influence of ferrite recrystallization and rapid spheroidization of cementite in the deformed pearlite on the formation and distribution of austenite in intercritically annealed C-Mn-Si steel. In this case, austenite forms initially on grain boundaries of elongated ferrite grains and later, *i.e.*, after completion of recrystallization, on carbides in the ferrite matrix.

Despite these important findings and their potential practical relevance, there is still a lack of detailed quantification on how heating rate will affect the austenite transformation during the isothermal portion of intercritical soaking. Thus, a systematic experimental study has been conducted to investigate the potential interaction of ferrite recrystallization and austenite formation kinetics at the intercritical temperatures for a variety of controlled heating rates for two cold-rolled steels with chemistries typically used for dual-phase and TRIP steels.

II. EXPERIMENTAL METHODOLOGY

This study examined two steel chemistries, one typical of a dual-phase steel and the other typical of a classical TRIP steel. The chemical composition of the two steels is given in Table I. Samples with a chemistry typical of a dual-phase steel, subsequently referred to as the Fe-C-Mn-Mo steel, were received from STELCO Inc. in both the hot-rolled and cold-rolled state. The hot-rolled and cold-rolled sheets had thicknesses of 3.8 and 1.5 mm, respectively, and the level of cold reduction was 55 pct.

The steel with a chemistry typical of a TRIP steel, subsequently referred to as the Fe-C-Mn-Si steel, was obtained from a 50-kg laboratory casting, which was subsequently hot-forged to a bar of 50 × 50 × 200 mm. The as-received material was cut into samples of 12.7-mm thickness and then hot rolled to 3-mm thickness in a laboratory scale hot-rolling mill at a temperature of 950 °C followed by air cooling. The hot-rolled steel was then given 50 pct cold reduction, resulting in a 1.5-mm-thick sample.

For recrystallization and austenite formation studies, test coupons of 10 × 60 × 1.5 mm were machined from the sheets with the longitudinal direction of the test coupon being aligned with the rolling direction. The Gleeble 1500 thermal-mechanical simulator (Dynamic Systems, Inc., Poestenkill, NY) was employed for all heat treatments. In particular, an excellent control of heating rate and sample temperature can be attained. The temperature was controlled using a type K thermocouple spot-welded on the center of the sample and all annealing tests were conducted under a rough vacuum, *i.e.*, ~26 Pa (2.0×10^{-1} Torr). To study recrystallization under isothermal conditions, the samples were heated at a rate of 50 °C/s to the desired annealing temperature. After a predetermined isothermal annealing time was reached, the sample was cooled to room temperature using a helium gas quench. The average cooling rate between the holding temperature and 250 °C was approximately 100 °C/s. After isothermal recrystallization experiments, the recrystallization behavior of the steels was studied under continuous heating conditions by heating the samples at various heating rates and quenching out.

For the austenite formation study, both the hot-rolled and cold-rolled samples were investigated. Two types of heating experiments were conducted: (1) continuous heating experiments were conducted at heating rates of 1 °C/s, 10 °C/s, and 100 °C/s and (2) experiments where the samples were heated into the intercritical region at various heating rates (1 °C/s, 10 °C/s, and 100 °C/s) and then held for a predetermined time at a given temperature. For both cases, the progression of the phase transformation was characterized by a dilatometer, which was attached onto the sample to measure the change in width during the heat treatment cycle. For the tests that involved holding in the intercritical region, the samples were then, after the appropriate isothermal hold time, heated to 1000 °C to enable the analysis of the dilation data to be conducted. The volume fraction of the austenite phase was obtained by analyzing the dilatometric data using the lever rule,[23] as depicted in Figure 1. Here, a straight line (AA') was fitted to the first linear portion of the dilation curve due to the ferrite/pearlite thermal expansion, while another straight line (FF') was fitted to the second linear portion of the dilation curve due to the thermal expansion of austenite. A vertical line can be drawn perpendicular to the temperature axis to determine the austenite volume fraction.

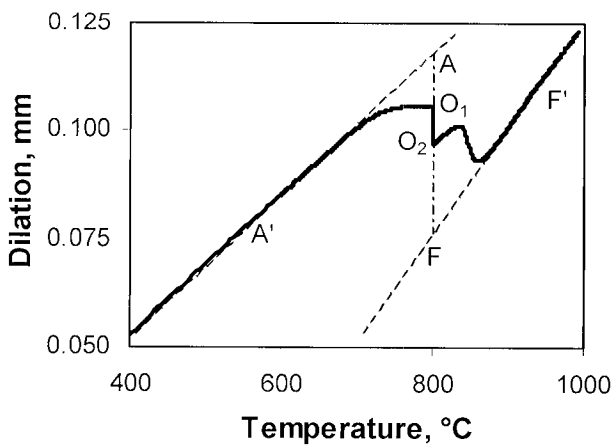

Fig. 1—Determination of austenite volume fraction from dilatometric data.

Table I. Chemical Composition of the Investigated Steels (Weight Percent)

Steel	C	Mn	Mo	Si	Ti	Nb	V	Cr	Ni	Cu	P	S	Ca	Al
Fe-C-Mn-Mo	0.06	1.86	0.155	0.077	0.011	0.002	0.004	0.048	0.014	0.015	0.015	0.0041	0.0012	0.043
Fe-C-Mn-Si	0.178	1.55	0.005	1.70	0.004	0.002	0.002	0.016	0.015	0.042	0.007	0.005	0.0013	0.026

When the intercritical holding temperature is reached, the austenite volume fraction is given by

$$V_\gamma(1) = AO_1/AF \quad [1a]$$

and at the end of holding at this temperature, it has increased to

$$V_\gamma(2) = AO_2/AF \quad [1b]$$

For microstructure analysis, additional samples were used and then these were quenched using helium gas after the appropriate heat treatment.

The microstructures of all samples (*i.e.*, as-received materials, samples of recrystallization, and intercritical annealing tests) were examined using optical microscopy. Samples were cut in the rolling plane to be analyzed and then mounted, mechanically grounded and polished, with the final polishing step using 0.05-μm silica solution. The etching procedure used for both materials was as follows: 3 seconds pre-etching in 2 pct nital, rinse in water, and final etching for 25 seconds in 10 pct sodium meta-bisulfite aqueous solution. The ferrite grain size was determined using the Jeffries method according to ASTM standard E112-96. The volume fraction of pearlite or martensite was determined using a Clemex image analysis system. The softening of ferrite was quantified by microhardness (Hv) measurements in the ferrite phase using a MICROMET3 (Buehler, Ltd., Lake Bluff, Illinois) microhardness tester under a load of 25 g. In addition, the ferrite recrystallization was measured metallographically, where ferrite grains with an aspect ratio smaller than 3 were considered recrystallized grains.

III. RESULTS

A. *Starting Microstructure and the Effect of Cold Rolling*

The microstructures of the as-received hot- and cold-rolled steels are shown in Figure 2. It can be observed that the hot-rolled steels feature a banded microstructure, *i.e.*, pearlite bands in a recrystallized ferrite matrix. The ferrite grain size is 6 and 11 μm for the Fe-C-Mn-Mo and Fe-C-Mn-Si steels, respectively. Quantitative metallography gives the pearlite volume fraction of 11 pct for the hot-rolled Fe-C-Mn-Mo steel and 25 pct for the hot-rolled Fe-C-Mn-Si steel. After cold rolling, the aspect ratio of the ferrite grains is consistent with the macroscopic level of cold reduction. Further, the pearlite colonies are also elongated, suggesting that ferrite and pearlite co-deform, as has also been reported in other studies.[20] The average pearlite band spacing for the hot-rolled and cold-rolled Fe-C-Mn-Mo steel is 31 and 15 μm, respectively, while for the hot- and cold-rolled Fe-C-Mn-Si steel, the spacing is 49 and 27 μm, respectively. The reduction in pearlite band spacing is also consistent with the macroscopic deformation level for these two steels.

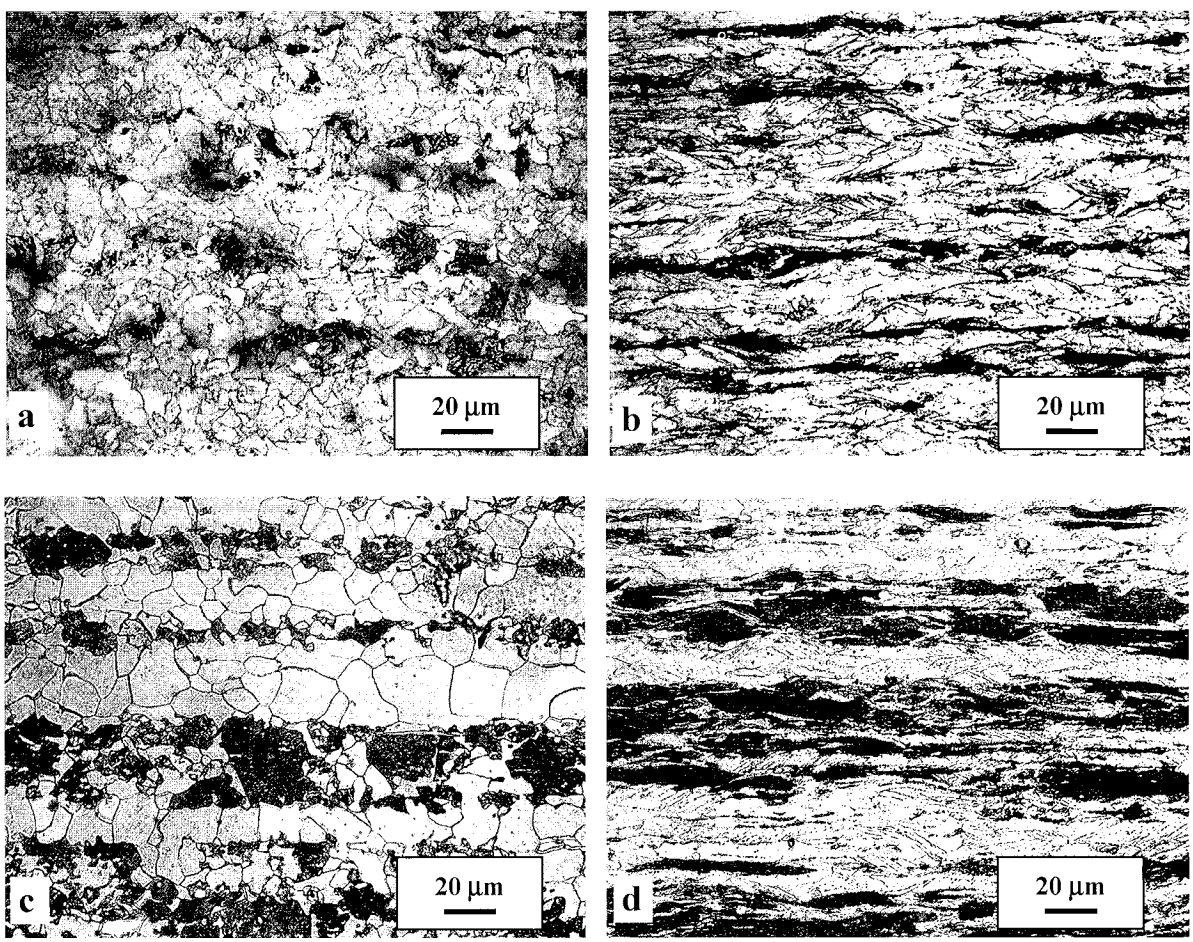

Fig. 2—Microstructures for the (*a*) hot-rolled and (*b*) 55 pct cold-rolled Fe-C-Mn-Mo steel, and (*c*) hot-rolled and (*d*) 50 pct cold-rolled Fe-C-Mn-Si steel; pearlite: dark; and ferrite: gray.

B. *Recrystallization of Ferrite*

During recrystallization, the deformed ferrite grains are replaced by equiaxed grains, as illustrated in Figure 3, for annealing at 650 °C for the Fe-C-Mn-Mo steel. Closer observation under the scanning electron microscope indicates that spheroidization of pearlite also occurs as the holding time increases. The recrystallized ferrite grain sizes were observed to increase from 6.3 to 8.9 μm when the recrystallization temperature was increased form 600 °C to 710 °C (Table II).

The fraction softening of ferrite can be obtained from the hardness; *i.e.*,

$$X = \frac{H_0 - H}{H_0 - H_{Rex}} \quad [2]$$

where H_0 is the initial microhardness of ferrite in the as-cold-rolled steel, H the microhardness after a given annealing condition, and H_{Rex} the microhardness corresponding to fully recrystallized steel. The softening of ferrite obtained from microhardness measurement can then be compared to the fraction recrystallized from quantitative metallography, as shown in Table III. The results from the two techniques indicate that the softening and fraction recrystallized are well correlated; *i.e.*, recovery appears to be a negligible softening process in these materials. Thus, hardness measurements can be used to determine the fraction recrystallized using Eq. [2].

The experimental isothermal recrystallization kinetics for the ferrite phase in Fe-C-Mn-Mo and Fe-C-Mn-Si steels based on this softening analysis are shown in Figure 4. A

Table II. Recrystallized Ferrite Grain Size for the Fe-C-Mn-Mo Steel

Isothermal annealing temperature, °C	600	650	680	710
Recrystallized ferrite grain size, μm	6.3	7.2	8.8	8.9

Table III. Comparison of the Ferrite Recrystallization Kinetics Determined by Microhardness Measurements and Quantitative Metallography for the Cold-Rolled Fe-C-Mn-Mo Steel Annealed at 680 °C

	Fraction Recrystallized	
Isothermal Annealing Time, s	Results from Microhardness Measurement	Results from Quantitative Metallography
10	0	0
30	0.15	0.16
60	0.48	0.47
180	0.74	0.72
300	0.82	0.80
600	1	1

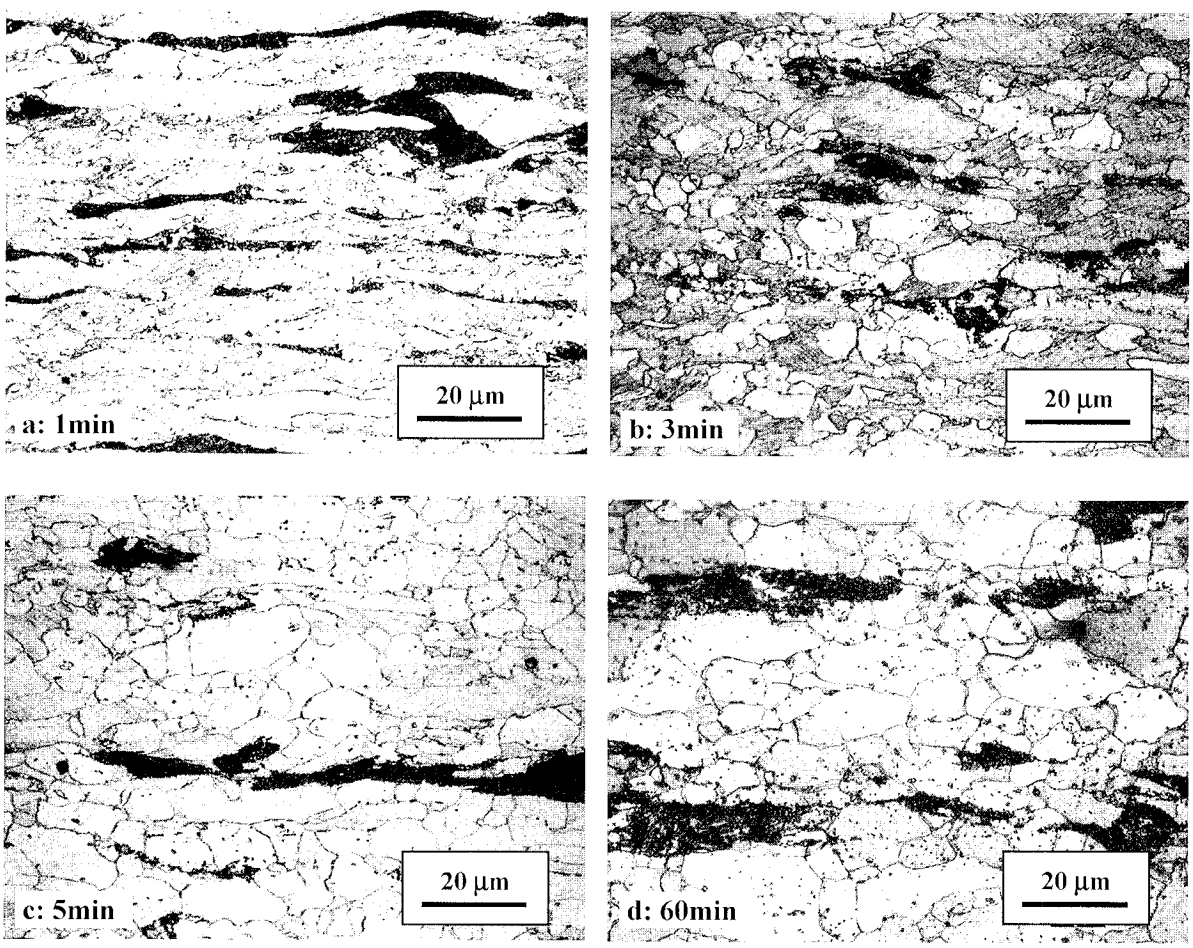

Fig. 3—Microstructure evolution for the cold-rolled Fe-C-Mn-Mo steel during isothermal annealing at 650 °C; pearlite: dark; and ferrite: gray.

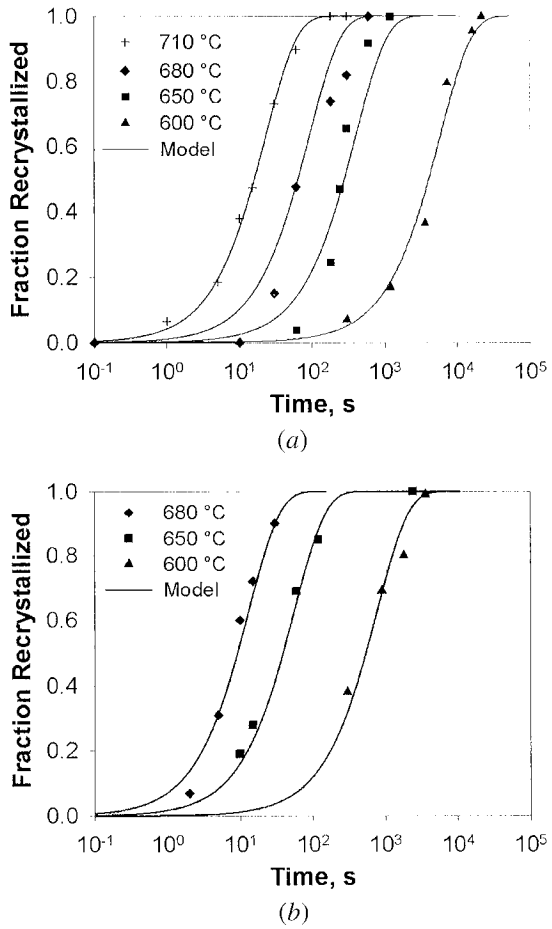

Fig. 4—Recrystallization kinetics and model predictions for the (*a*) Fe-C-Mn-Mo and (*b*) Fe-C-Mn-Si steel.

suitable fit to the experimental results can be obtained using the Avrami equation,[24,25] *i.e.*,

$$X = 1 - \exp(-bt^n) \quad [3]$$

where X is the volume fraction recrystallized and n and b are adjustable parameters where

$$b = b_o \exp\left(\frac{-Q}{RT}\right) \quad [4]$$

describes the temperature dependence. Here, b_o is a constant and Q is an effective activation energy for the recrystallization process. For both steels, a good fit to the data can be found with $n = 1$ and $Q = 350$ kJ/mol. However, the recrystallization rates are higher for the Fe-C-Mn-Si steel, and this is reflected in the values for b_o; *i.e.*, $b_o = 1.6 \times 10^{18}$ s^{-1} for the Fe-C-Mn-Si steel compared to $b_o = 7.2 \times 10^{16}$ s^{-1} for the Fe-C-Mn-Mo steel.

An apparent activation energy of 350 kJ/mol is considerably larger than the activation energy of 251 kJ/mol for self-diffusion in bcc-iron[26] and 226 kJ/mol reported by Yang and co-workers[20] for 50 pct cold-rolled low C-Mn steel. This can be understood in terms of the effects of solute additions such as Mn[27,28] and Mo,[29] which have been shown to delay the growth of newly recrystallized grains due to solute drag on migrating grain boundaries. The difference in the rate of recrystallization for the Fe-C-Mn-Mo and the Fe-C-Mn-Si steel is summarized in Figure 5, which shows the time for 50 pct recrystallization *vs*

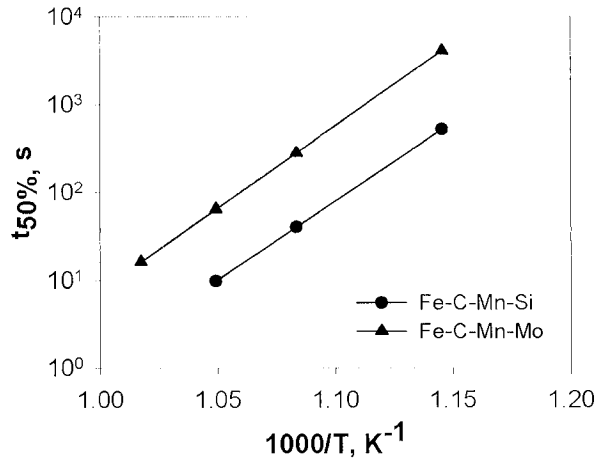

Fig. 5—Time for 50 pct recrystallization as a function of temperature.

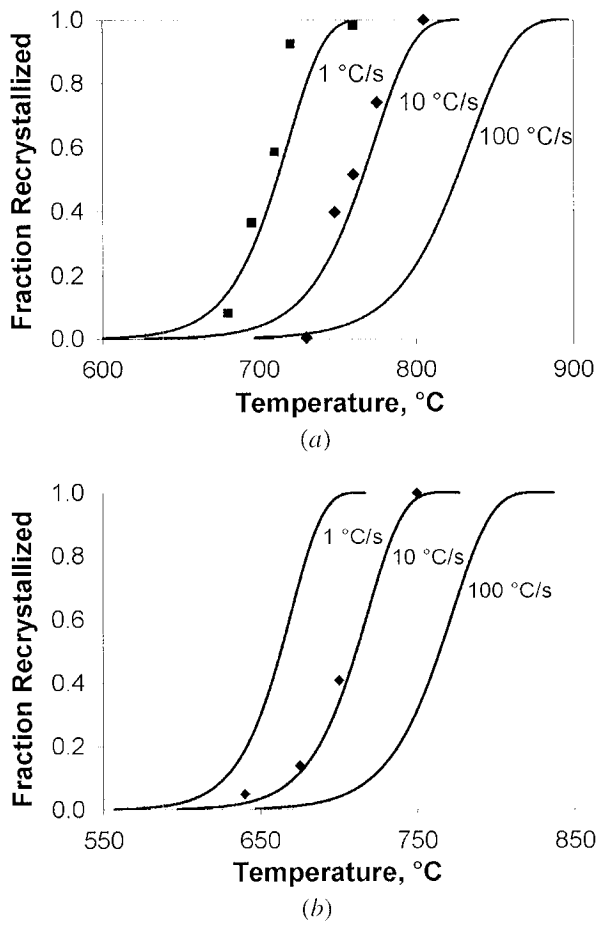

Fig. 6—Recrystallization behavior for (*a*) Fe-C-Mn-Mo steel and (*b*) Fe-C-Mn-Si steel under continuous heating conditions; symbols represent experimental data and lines represent model predictions.

temperature. The slower rate of recrystallization in the Fe-C-Mn-Mo steel can be attributed to a particularly strong solute drag effect of Mo, which is well documented for austenite recrystallization[30] and the austenite-to-ferrite transformation.[31] To examine recrystallization under nonisothermal conditions, experiments were conducted at constant heating rates where the samples were quenched at various temperatures. Figure 6 shows the results for fraction recrystallized based on Eq. [2].

The solid lines are the predictions from applying Eq. [3] in differential form and then numerically integrating.[32] Good agreement can be observed between the model and experiments for heating rates of 1 °C/s and 10 °C/s and the predictions for 100 °C/s are also shown in Figure 6.

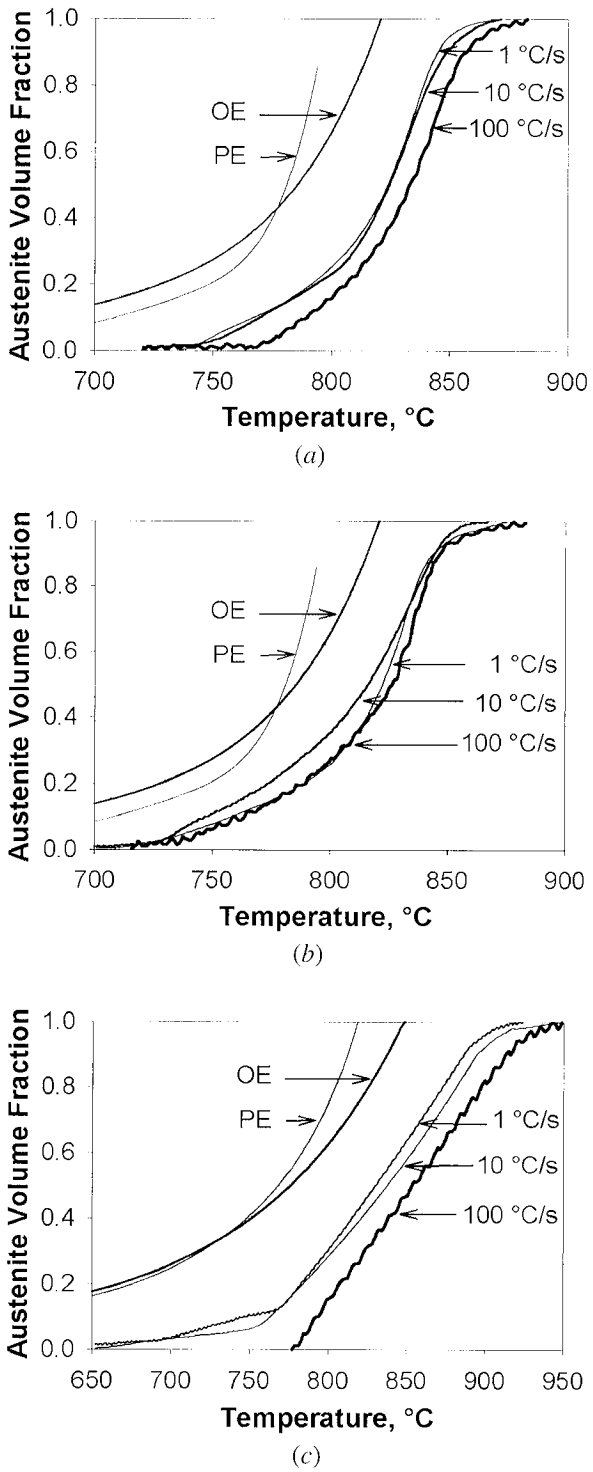

Fig. 7—Austenite formation kinetics for the (*a*) hot-rolled and (*b*) cold-rolled Fe-C-Mn-Mo steel; and (*c*) cold-rolled Fe-C-Mn-Si steel under continuous heating conditions and orthoequilibrium (OE) and paraequilibrium (PE) austenite fractions.

C. *Austenite Formation*

1. *Continuous heating tests*

The results for the austenite formation kinetics under continuous heating condition (1 °C/s, 10 °C/s, and 100 °C/s) for the hot-rolled and cold-rolled Fe-C-Mn-Mo and cold-rolled Fe-C-Mn-Si steels are summarized in Figure 7. In addition to the experimental results, the orthoequilibrium and paraequilibrium austenite volume fraction calculated from Thermo-Calc (Thermo-Calc Software, Stockholm, Sweden) using the FE-2000 database are shown for comparison (note: paraequilibrium denotes a constraint equilibrium without partitioning of substitutional alloying elements). For the hot-rolled Fe-C-Mn-Mo steel (Figure 7(a)), there is no significant difference in the kinetics of austenite formation for heating rates of 1 °C/s and 10 °C/s. However, the austenite fraction clearly falls significantly below equilibrium for all temperatures. Increasing the heating rate to 100 °C/s results in the expected behavior; *i.e.*, the amount of austenite fraction at a given temperature is decreased.

The results for the cold-rolled Fe-C-Mn-Mo steel are shown in Figure 7(b). The significant observation to be noted here is that there is essentially no difference in the austenite transformation start and finish temperatures or the rate of austenite formation for all the heating rates investigated (1 °C/s, 10 °C/s, and 100 °C/s). However, the rate of austenite formation is increased for the cold-rolled Fe-C-Mn-Mo steel compared to the hot-rolled Fe-C-Mn-Mo steel.

For the cold-rolled Fe-C-Mn-Si steel, the observations on austenite formation are different from the cold-rolled Fe-C-Mn-Mo steel, as can be seen by comparing Figure 7(c) with Figure 7(b); *i.e.*, a significant difference is observed for a heating rate of 100 °C/s for the cold-rolled TRIP steel. This behavior is qualitatively similar to the austenite formation behavior observed in the hot-rolled Fe-C-Mn-Mo steel Figure 7(a) *i.e.*, the degree of austenite transformed at a given temperature is decreased for the highest employed heating rate (100 °C/s).

2. *Ramp and hold tests*

To examine the effect of heating rate in more detail, a series of annealing tests were conducted where the material was heated at different rates and then held isothermally at various temperatures in the intercritical region for 10 minutes. Figure 8 compares the results from the analysis of dilatometry data for

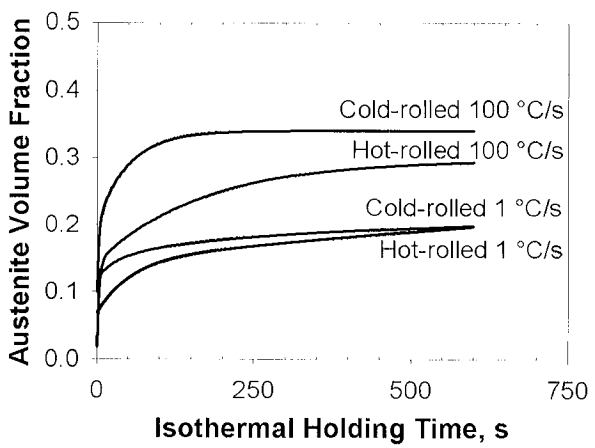

Fig. 8—Effect of initial heating rate on the isothermal austenite formation kinetics at 750 °C for hot-rolled and cold-rolled Fe-C-Mn-Mo steel.

heating rates of 1 °C/s and 100 °C/s to an isothermal hold at 750 °C for the hot- and cold-rolled Fe-C-Mn-Mo steel. Turning first to the hot-rolled material, one can see that the volume fraction of austenite phase increases with increased annealing time, as expected. However, the more interesting observation is that the samples with higher heating rates have a much higher austenite volume fraction for a given annealing time. For example, at the beginning of the isothermal hold, the fraction of austenite is 0.09 and 0.11 for the 1 °C/s and 100 °C/s heating rates, respectively, but these fractions increase to 0.21 and 0.29 after 10 minutes of holding at 750 °C. For the cold-rolled material, the effect of heating rate is even more significant. In this case, the fractions of austenite at the beginning of the isothermal hold are 0.12 and 0.14 for the 1 °C/s and 100 °C/s heating rates, respectively (*i.e.*, slightly higher than for the hot-rolled material). At the end of the isothermal hold, this difference increases to 0.17 and 0.34 for heating rates of 1 °C/s and 100 °C/s, respectively, *i.e.*, the final fraction of austenite is twice as high for the higher heating rate even though the initial fractions are essentially the same.

Figure 9 shows the corresponding microstructures for the cold- and hot-rolled Fe-C-Mn-Mo steels, which were heated at rates of 1 °C/s and 100 °C/s to a temperature of 750 °C, held for 10 minutes, and then helium quenched. In these micrographs, the light colored phase is ferrite and the dark phase is martensite. In examining these micrographs, it is assumed that the quench rate, which was greater than 100 °C/s, is sufficient to prevent any transformation of austenite back to ferrite, and thus, the austenite volume fraction and distribution at intercritical temperature are considered the same as those observed for martensite at room temperature. The results for austenite fraction after 10 minutes at 750 °C obtained from quantitative metallography and from the analysis of dilation data are shown in Table IV and are found to be in good agreement with each other. For example, in the hot-rolled steel, the volume fraction of austenite was measured to be 0.19 and 0.21 for 1 °C/s and 0.27 and 0.29 for 100 °C/s by metallography and dilatometry measurements, respectively. Similar agreement was found for the cold-rolled samples. Further, several important observations can be made regarding the distribution and morphology of austenite. For the hot-rolled steel heated to 750 °C at 1 °C/s (Figure 9(a)), relatively large austenite islands can be observed as well as

Table IV. Austenite Volume Fraction for the Fe-C-Mn-Mo Steel for Heating at Different Rates and Then Holding at 750 °C for 10 Minutes

Heating Rate °C/s	Austenite Volume Fraction			
	Hot-Rolled		Cold-Rolled	
	Metallography	Dilatometry	Metallography	Dilatometry
1	0.19	0.21	0.17	0.17
100	0.27	0.29	0.34	0.33

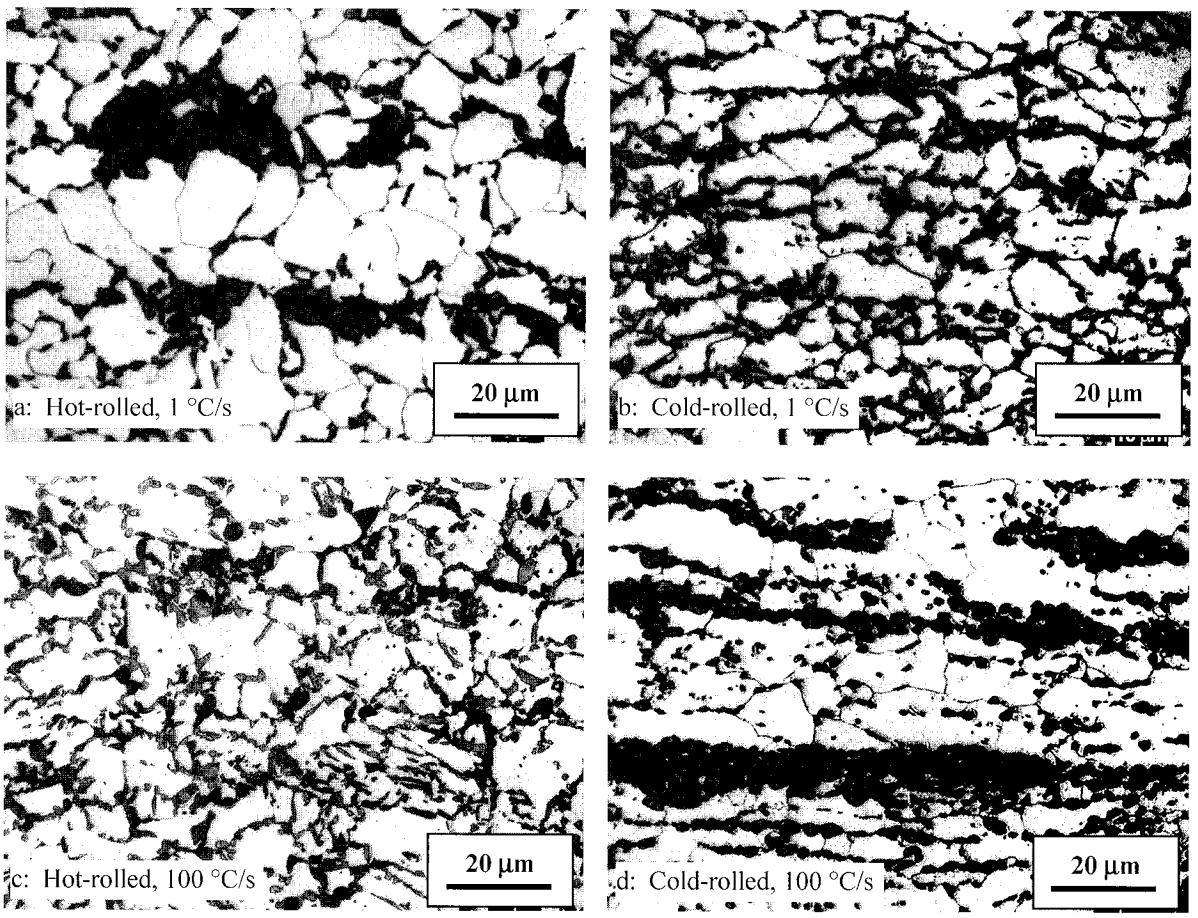

Fig. 9—Microstructures for the hot- and cold-rolled Fe-C-Mn-Mo steel isothermally annealed at 750 °C for 10 min with initial heating rates of 1 °C/s and 100 °C/s; martensite (austenite at intercritical temperature): dark; and ferrite: gray.

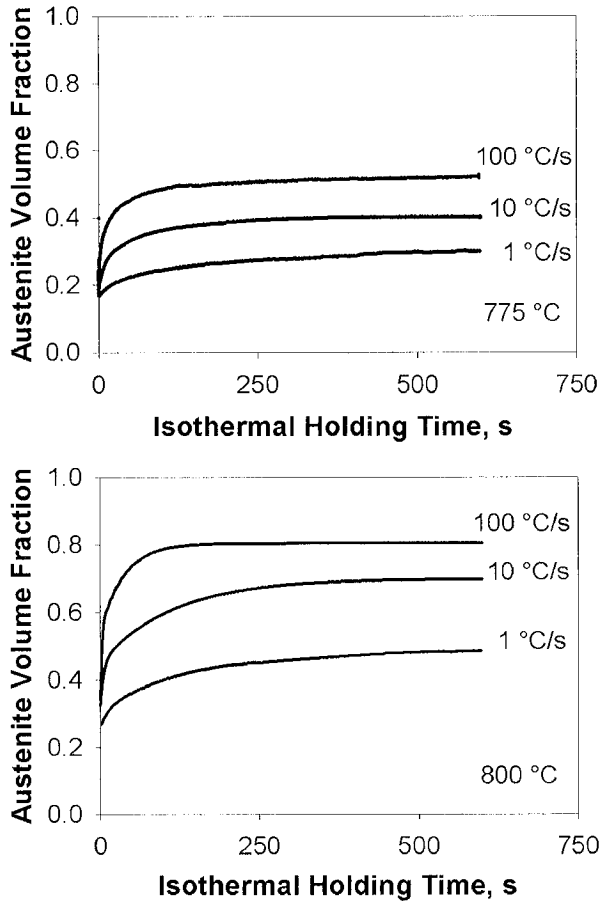

Fig. 10—Effect of initial heating rate on the austenite formation kinetics of cold-rolled Fe-C-Mn-Mo steel during holding at 775 °C and 800 °C, respectively.

a small number of much smaller islands distributed on the ferrite boundaries. When the heating rate for the hot-rolled steel is increased to 100 °C/s (Figure 9(c)), the austenite islands are smaller and form an almost complete necklace of grains along the ferrite grain boundaries. Turning to the initially cold-rolled materials, one can observe that at a heating rate of 1 °C/s (Figure 9(b)), some highly elongated austenite islands and a number of smaller islands on ferrite grain boundaries have been formed. The most striking microstructure is observed for the cold-rolled material with a heating rate of 100 °C/s. In this case, a relatively low density of large, highly elongated austenite islands form. In addition, only relatively few austenite grains can be seen on ferrite grain boundaries.

To further appreciate the transformation behavior in the cold-rolled Fe-C-Mn-Mo steel, Figure 10 shows the isothermal austenite formation kinetics at 775 °C/s and 800 °C with initial heating rates of 1 °C/s, 10 °C/s, and 100 °C/s. Similar to the transformation data at 750 °C, the transformation in the isothermal stage is strongly affected by the heating rate, *i.e.*, increasing the heating rate increases the transformation rate at holding temperature. The effects of heating rate and temperature are similar for the cold-rolled Fe-C-Mn-Si steel, as shown in Figure 11 for annealing at 750 °C and 785 °C with heating rates of 1 °C/s and 100 °C/s. It is worth noting that although significant differences have been observed in the austenite volume fraction after 10 minutes of isothermal

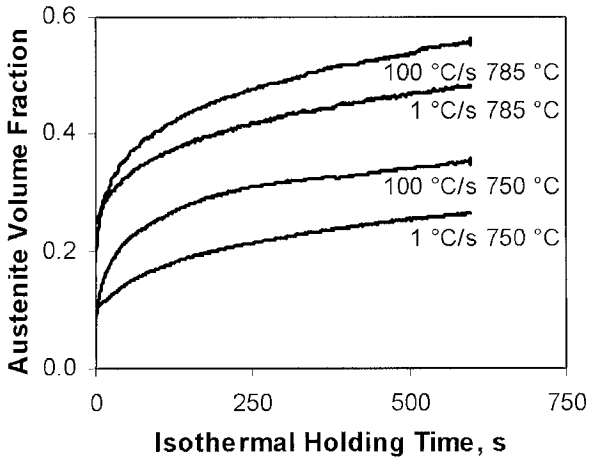

Fig. 11—Effect of initial heating rate on the austenite formation kinetics of the cold-rolled Fe-C-Mn-Si steel during holding at 750 °C and 785 °C, respectively.

holding for different initial heating rates (Figures 8, 10, and 11), these differences should eventually disappear; *i.e.*, given enough time, the material will reach the equilibrium austenite volume fraction at these intercritical temperatures regardless of the initial heating rate. In fact, careful examination of the data in Figure 8 or 10 indicates that the slope of the austenite fraction *vs* time curve after 10 minutes of holding for the low initial heating rates has a small positive value, clearly suggesting that 10 minutes of isothermal holding at these temperatures is not sufficient for the material to reach equilibrium condition.

IV. DISCUSSION

A. *Phenomenological Observations*

The microstructures of the hot-rolled Fe-C-Mn-Mo and Fe-C-Mn-Si steels feature pearlite colonies with a banded morphology surrounded by equiaxed ferrite grains. After cold rolling, the morphology of both phases becomes elongated; *i.e.*, the ferrite grains become elongated and contain deformation bands and other substructures, while the pearlite is also deformed, as seen in Figures 2(b) and (d). The cold work has the following effects on the material: (1) there is an increase in the stored energy of the material due to the high dislocation density and this provides the driving pressure for the ferrite recrystallization upon annealing;[33] (2) the total ferrite grain boundary area is increased; and (3) the cementite laminar structure in pearlite is broken down. The latter has been shown to promote spheroidization of cementite during subsequent annealing processes.[9,20]

Upon annealing of the cold-rolled material, the stored energy is released by recrystallization. In general, recrystallization of ferrite is completed before the intercritical temperature range is reached. However, for sufficiently high heating rates, ferrite recrystallization can be delayed to temperatures above the start temperature, T_S, at which austenite formation in ferrite was first experimentally observed as a function of heating rate (*i.e.*, after the rapid pearlite to austenite reaction, which corresponds, for example, to the first 11 pct transformed in the Fe-C-Mn-Mo steel). Figure 12 shows a comparison of the nonisothermal recrystallization

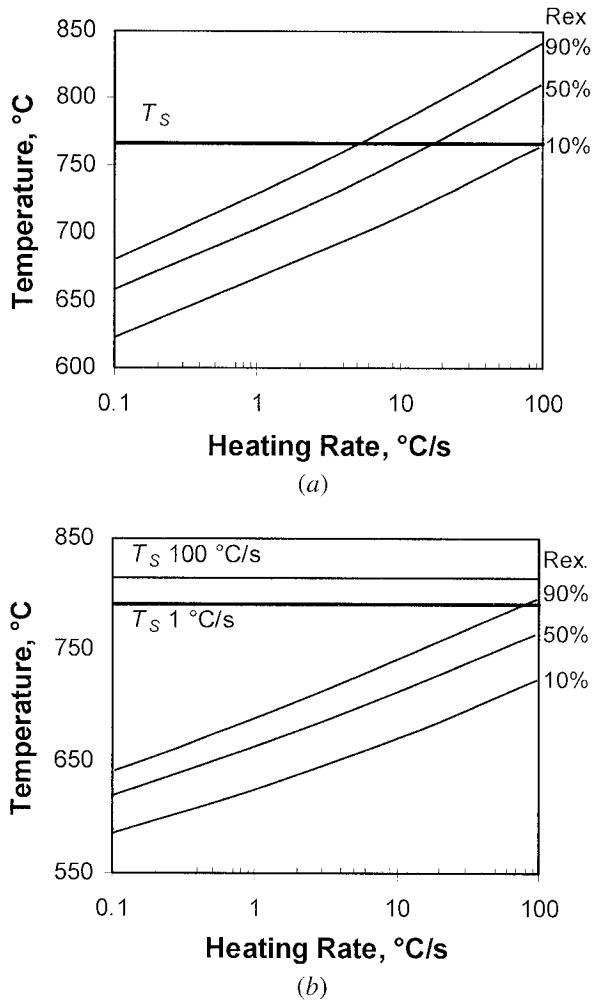

Fig. 12—Effect of heating rate on the progressing of recrystallization with respect to the onset of austenite formation for the (*a*) Fe-C-Mn-Mo steel and (*b*) Fe-C-Mn-Si steel.

kinetics derived using the model described in Section III–B and the temperature, T_S. For the Fe-C-Mn-Mo steel, it can be observed that there is a significant overlap between ferrite recrystallization and austenite formation at higher heating rates. For example, at heating rates of 10 °C/s and 100 °C/s, the ferrite is 50 and 90 pct unrecrystallized, respectively, when austenite formation in ferrite is first observed. On the other hand, Figure 12(b) shows that for the Fe-C-Mn-Si steel, ferrite recrystallization is completed before the austenite formation in ferrite starts for all investigated heating rates. Thus, for the Fe-C-Mn-Si steel, heating rates on the order of 1000 °C/s appear to be required for substantial overlap between ferrite recrystallization and austenite formation consistent with the recent experimental results of Petrov *et al.*[22] The fact that the overlap between recrystallization and austenite formation occurs at lower heating rates for the Fe-C-Mn-Mo steel is related to two observations: (1) recrystallization is slower in this steel and (2) T_S is lower. Both of these effects can be attributed to the differences in chemistry of the two steels, *i.e.*, (1) Mo delays recrystallization and (2) Si increases the A_{e1} temperature and thus also T_S.

It might be expected that there would be important implications on the formation of austenite when it occurs simultaneously with ferrite recrystallization, as will be discussed subsequently. However, the effect of heating rate on the subsequent isothermal transformation was also observed for hot-rolled material, *i.e.*, in the absence of recrystallization. Thus, it appears that there is an important intrinsic effect of thermal history on austenite formation, *i.e.*, the reaction is not additive.

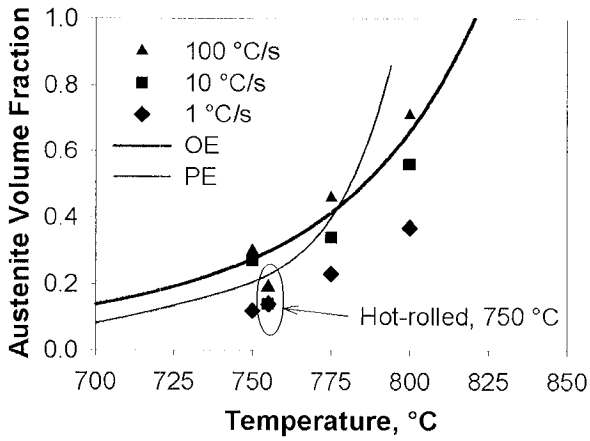

Fig. 13—Summary of austenite fractions in the Fe-C-Mn-Mo steel for 1 min of holding at various temperatures after different heating rates to holding temperature, and orthoequilibrium (OE) and paraequilibrium (PE) fractions.

Figure 13 summarizes the volume fraction of austenite for the Fe-C-Mn-Mo steel after 1 minute of holding at various temperatures with different heating rates being employed to reach the temperature. The experimental results are compared to ortho- and paraequilibrium predictions from Thermo-Calc. The limited results from the hot-rolled steel annealed at 750 °C are also presented. The latter results show a similar trend as those for the cold-rolled material, although to a smaller degree. As the heating rate increases, a larger fraction of austenite is obtained after the same isothermal holding time. All the other trends of the results shown in Figure 13 are consistent with expectations, *i.e.*, the volume fraction of austenite increases with annealing temperature. The largest observed austenite fractions appear to coincide with orthoequilibrium predictions. However, this should not be mistaken as proof that redistribution of substitutional alloying elements has taken place. At lower temperatures (*i.e.*, <775 °C), ortho- and paraequilibrium yield similar austenite fractions. On the other hand, at higher temperatures, the austenite fraction in paraequilibrium is significantly larger than that in orthoequilibrium. Further, using the diffusion data reported for Mn,[134] typical diffusion distances for a holding time of 1 minute in the temperature range 750 °C to 800 °C are estimated to be 0.2 μm in ferrite and less than 0.01 μm in austenite. This estimate replicates the detailed austenite growth analysis by Wycliffe *et al.*[113] Their analysis predicts some Mn partitioning such that a nonuniform Mn distribution is established in relatively short times. However, much longer holding times on the order of hours would be required to obtain complete redistribution. A previous study on a 0.2 wt pct carbon steel has shown that this process can take more than 14 hours to complete.[135]

B. *Proposed Mechanisms*

To appreciate the role of heating rate, it is worthwhile to recall the basic phenomena of the austenite formation, which is a diffusional transformation occurring by nucleation and

growth. The transformation starts from the pearlite colonies by nucleation at the cementite-ferrite interface followed by quick growth consuming the dissolving pearlite. Subsequently, austenite may nucleate at ferrite grain boundaries in competition with austenite growth from the prior pearlite areas. It appears that the competition between austenite formed at these different sites is responsible for the marked heating rate effect on the transformation kinetics. Slower heating rates will favor substantial growth of austenite nucleated at pearlite sites, whereas faster heating rates will promote additional nucleation at ferrite grain boundaries. Re-examination of the microstructures shown in Figure 9 appears to support this general trend for the hot-rolled material but not for the cold-rolled steel.

Figure 14 is a schematic diagram that can be used to rationalize the formation of the microstructural features observed in Figure 9. Starting with the hot-rolled material at a heating rate of 1 °C/s, relatively large austenite islands are observed and there appears to be a substantial amount of ferrite boundaries free of austenite. The distribution of these islands follows the distribution of pearlite in the as-hot-rolled material and shows that essentially the entire initial pearlite colony is transformed to austenite. For this heating rate, grain boundary– and pearlite-nucleated austenite remain distinct and compete during growth. In particular, C has to diffuse from the areas of growing pearlite-nucleated austenite over relatively large distances to facilitate growth of grain boundary austenite. This competition contributes to the comparatively slow transformation rates during holding. For the hot-rolled material at a heating rate of 100 °C/s, the extent of austenite nucleation at ferrite grain boundaries is such that an almost complete network of austenite along the boundaries connecting to the pearlite-nucleated austenite emerges. Thus, there is no growth com-

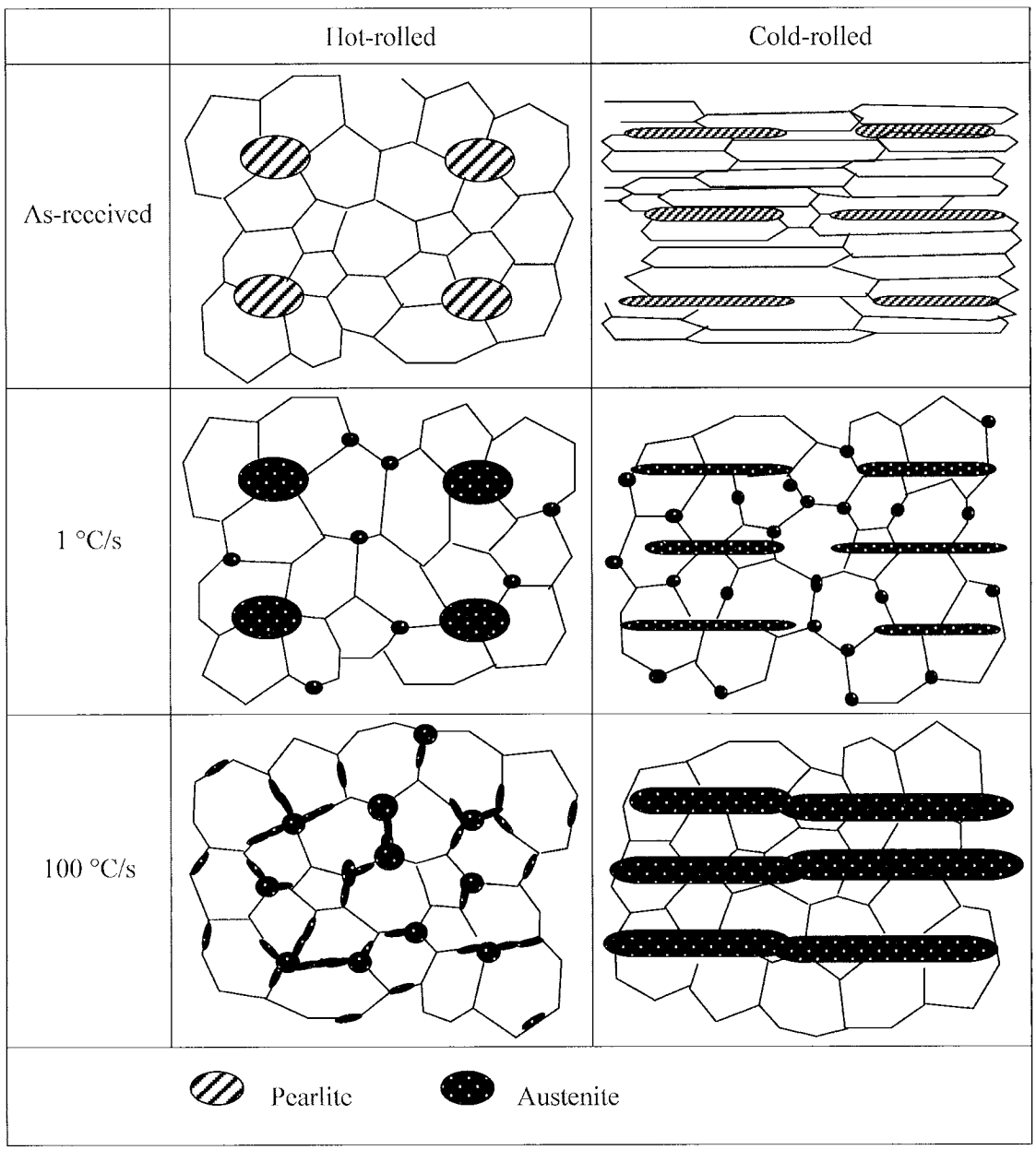

Fig. 14—Schematic illustration for the microstructure evolution of cold-rolled Fe-C-Mn-Mo steel annealed with different heating rates to holding temperature.

petition between pearlite- and grain boundary–nucleated austenite, thereby promoting larger transformation rates at holding temperature. The higher transformation rates for this condition are also consistent with the larger ferrite-austenite interfacial area associated with the observed austenite morphology.

In the case of the cold-rolled sample, the situation is different for a number of reasons. First, the distribution and shape of the pearlite colonies (where the majority of the carbon is located) have been geometrically modified by cold rolling. Second, at the higher heating rates, recrystallization occurs concurrent with austenite nucleation. At the lowest heating rate (1 °C/s), it has been shown that recrystallization of ferrite is essentially complete before austenite nucleation occurs (Figure 12). This situation can then be expected to resemble that of the hot-rolled sample. Indeed the kinetics of austenite formation is quite similar, as shown in Figure 8. However, the morphology of the austenite is different due to the fact that the shape of the initial pearlite colonies has been substantially modified by the cold rolling process.

The most complex situation is the one where the cold-rolled material experiences the highest heating rate (*i.e.*, 100 °C/s). In this case, much larger elongated austenite islands are observed. The shape and geometric arrangement of these islands corresponds to the as-rolled pearlite distribution; however, the austenite islands are considerably larger. Moreover, there is a striking absence of austenite formed at ferrite grain boundaries. The absence of austenite on ferrite grain boundaries can be understood as follows. The sequence of micrographs shown in Figure 15 clearly illustrates that ferrite is still recrystallizing when austenite has nucleated in the pearlite colonies and starts to grow from there. Subsequently, these moving ferrite grain boundaries do not provide suitable nucleation sites for austenite. Thus, there are only a very few austenite particles located at the ferrite grain boundaries. The pearlite-nucleated austenite can then grow without significant competition from grain boundary austenite. This growth is apparently fast enough to eliminate the driving pressure required for austenite nucleation at ferrite grain boundaries before the completion of ferrite recrystallization. Under these conditions, austenite growth occurs rapidly by thickening and lengthening of the former pearlite colonies since only comparatively short-range carbon redistribution over the thickness of the pearlite-nucleated austenite is necessary for growth. Indeed, the fastest austenization formation rates are observed for this condition. As a result, a blocklike austenite distribution forms parallel to the rolling direction with the largest transformation rate of the four considered cases.

This interpretation appears to be in contrast to that of Yang *et al.*,[20] who also found austenite bands parallel to the rolling direction but attributed them to austenite nucleation primarily occurring on ferrite grain boundaries before completion of recrystallization. Closer inspection of their results suggests that these locations coincide with the presence of spheroidized cementite colonies along the boundaries of the elongated ferrite grains; *i.e.*, as proposed here, preferred nucleation at the pearlite-ferrite and cementite-ferrite interfaces appears to occur.

The same principles explain the unusual austenite formation behavior under continuous heating conditions (Figure 7). In the hot-rolled material, increasing the heating rate leads to an enhanced austenite nucleation at ferrite boundaries. Associated with this is a gradual decrease of growth competition between pearlite- and grain boundary–nucleated austenite until a network connecting the different types of austenite is formed, *i.e.*, the growth geometry changes for intermediate heating rates. As a result, the temperature dependence of the fraction transformed is similar for heating rates of 1 °C/s and 10 °C/s, and only for even higher heating rates is the transformation delayed to higher temperatures, as expected from a diffusional transformation with a given growth geometry. The interaction of recrystallization and austenite formation in the cold-rolled Fe-C-Mn-Mo steel for higher heating rates (>10 °C/s) extends

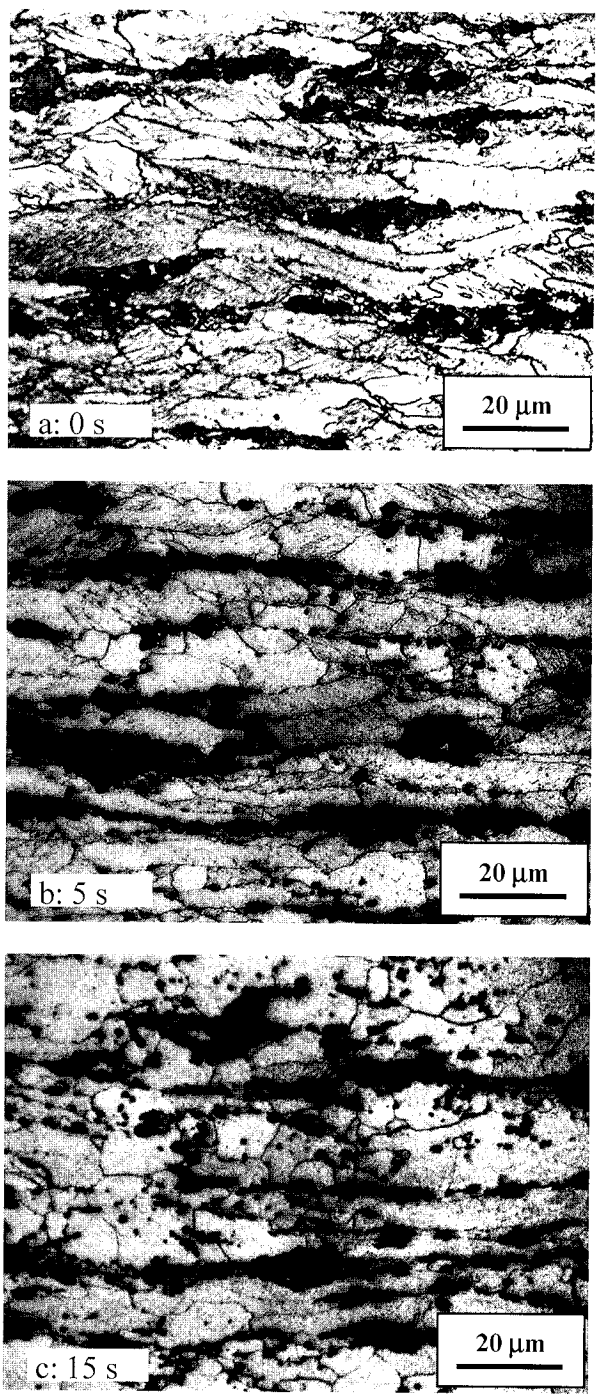

Fig. 15—Microstructure evolution for the cold-rolled Fe-C-Mn-Mo steel annealed at 750 °C with an initial heating rate of 100 °C/s.

the apparent heating rate independence of the transformed austenite fraction to even higher heating rates, *i.e.*, 100 °C/s.

The latter is not observed for the cold-rolled Fe-C-Mn-Si steel. As indicated in Figure 12, ferrite recrystallization is sufficiently fast that no overlap with austenite formation occurs at the highest investigated heating rate of 100 °C/s. Consequently, the Fe-C-Mn-Si steel displays, in the investigated heating rate range, trends in terms of austenite formation similar to those of the hot-rolled Fe-C-Mn-Mo steel.

The discussion so far has focused on the ferrite-to-austenite transformation. However, there are also important implications of the heat-treatment path on the pearlite-to-austenite formation transformation, which precedes the ferrite-to-austenite transformation. This can be seen for the case of the Fe-C-Mn-Si steel intercritically annealed at 750 °C, where even when initially the austenite fraction remains below the pearlite fraction of 25 pct, a clear heating rate dependence is found. It can be expected that slower heating rates promote spheroidization of pearlite. The early work of Roberts and Mehl[4] found that spheroidized pearlite transforms to austenite more slowly than unspheroidized pearlite, which is consistent with the observations made in the current work (Figure 11).

V. SUMMARY AND CONCLUSIONS

The present work represents an experimental study to examine the effect of heating rate on austenite formation for steels with chemistries typically used for dual-phase and TRIP steels. Very significant effects of heating rate on both the fraction of austenite and its spatial distribution and morphology have been observed. These observations are of importance since intercritical annealing represents the first processing step during annealing of dual-phase or TRIP steels. The microstructure produced in this step is inherited through the remainder of the process and is thus reflected in the final microstructure. The work raises a number of issues that are of interest both from a fundamental point of view and from the perspective of opportunities in alloy design and industrial processing.

Fundamentally, heating rate clearly affects the nucleation and growth of austenite both for hot-rolled and cold-rolled materials, although the effect is greater for cold-rolled materials. The interaction between the microstructure of the ferrite/pearlite mixture and austenite formation is complex and requires further understanding. The basic trends can be rationalized by the competing mechanisms for nucleation and growth of austenite and how these depend on the starting microstructure (*i.e.*, spatial distribution of pearlite and the degree of ferrite recrystallization). The interaction between ferrite recrystallization and austenite formation is strong, and it affects not only the kinetics of austenite formation but also the spatial distribution and morphology of austenite. The effects of various nucleation scenarios and growth geometries can, for example, be examined using the phase field approach.[36] Thus, phase field modeling is currently being applied to rationalize the observed austenite formation kinetics in more detail.

From an industrial point of view, the range of heating rates examined, (1 °C/s to 100 °C/s), are typical of continuous annealing lines used for galvanizing such that these effects are expected to be of industrial relevance. The morphology of the final microstructure is of particular interest since the highly anisotropic martensite distribution that is produced under high heating rates from cold-rolled starting materials is expected to have significant effects on the final mechanical properties. Further, it appears that it is possible to tailor microstructures by control of processing conditions and alloy design. The level of cold rolling is expected to be important since it determines the initial spatial distribution of carbon, which is predominately found in the pearlite islands and will also effect the rate of ferrite recrystallization. The interaction between ferrite recrystallization and austenite formation can be controlled by changing heating rates but also by alloy design. For example, the addition of elements such as Mo, Nb, or B, which are known to retard ferrite recrystallization, would promote the overlap between these phenomena.

ACKNOWLEDGMENTS

The authors are grateful to the Natural Sciences and Engineering Research Council of Canada (NSERC) and STELCO Inc. for the financial support. Mr. Fateh Fazili is acknowledged for helping with Thermo-Calc calculations and Mr. Rick Adam for helping with experimental measurements. The discussions with Dr. Farid Hassani are greatly appreciated.

REFERENCES

1. P. Jacques, X. Cornet, P. Harlet, J. Ladriere, and F. Delannay: *Metall. Mater. Trans. A*, 1998, vol. 29A, pp. 2383-93.
2. G.R. Speich and R.L. Miller: in *Structure and Properties of Dual-Phase Steels*, AIME, New York, NY, 1979, pp. 13-22.
3. J.O. Arnold and A. McWilliams: *J. Iron Steel Inst.*, 1905, No. 2, pp. 352.
4. G.A. Roberts and R.F. Mehl: *Trans. ASM*, 1943, vol. 31, pp. 613-50.
5. C.I. Garcia and A.J. DeArdo: *Metall. Trans. A*, 1981, vol. 12A, pp. 521-30.
6. G.R. Speich, V.A. Demarest, and R.L. Miller: *Metall. Trans. A.*, 1981, vol. 12A, pp. 1419-28.
7. R.D. Lawson, D.K. Matlock, and G. Kraus: in *Fundamentals of Dual-Phase Steels*, R.A. Kot and B.L. Bramfitt, eds., AIME, New York, NY, 1981, pp. 347-81.
8. U.R. Lenel: *Scripta Metall.*, 1983, vol. 17, pp. 471-74.
9. J.J. Yi, I.S. Kim, and H.S. Choi: *Metall. Trans. A*, 1985, vol. 16A, pp. 1237-45.
10. R.C. Reed, T. Akbay, Z. Shen, J.M. Robinson, and J.H. Root: *Mater. Sci. Eng. A.*, 1998, vol. 256, pp. 152-65.
11. W.J. Kaluba, R. Taillard, and J. Foct: *Acta Mater.*, 1998, vol. 46, pp. 5917-27.
12. J.D. Puskar, R.C. Dykhuizen, C.V. Robino, M.E. Burnett, and J.B. Kelley: in *41st Mechanical Working and Steel Processing Conf. Proc.*, ISS, Warrendale, PA, 1999, vol. XXXVII, pp. 625-35.
13. P. Wycliffe, G.R. Purdy, and J.D. Embury: in *Fundamentals of Dual-Phase Steels*, R.A. Kot and B.L. Bramfitt, eds., AIME, New York, NY, 1981, pp. 59-83.
14. S.K. Nath, S. Ray, V.N.S. Mathur, and M.L. Kapoor: *Iron Steel Inst. Jpn. Int.*, 1994, vol. 34, pp. 191-97.
15. C. Atkinson, T. Akbay, and R.C. Reed: *Acta Mater.*, 1995, vol. 43, pp. 2013-31.
16. C. Garcia, F.G. Caballero, C. Capdevila, and H.K.D.H. Bhadeshia: *Scripta Mater.*, 1998, vol. 39, pp. 791-96.
17. A. Jacot, M. Rappaz, and R.C. Reed: *Acta Mater.*, 1998, vol. 46, pp. 3949-62.
18. R. Mancini and C. Budde: *Acta Mater.*, 1999, vol. 47, pp. 2907-11.
19. S.W. Thompson, G.S. Fan, and P.R. Howell: in *Phase Transform. Ferrous Alloys*, Proc. Int. Conf., A.R. Marder and J.I. Goldstein, eds., TMS–AIME, Warrendale, PA, 1984, pp. 43-47.
20. D.Z. Yang, E.L. Brown, D.K. Matlock, and G. Krauss: *Metall. Trans. A*, 1985, vol. 16A, pp. 1385-92.
21. S. Sekino and N. Mori: *Trans. Iron Steel Inst. Jpn.*, 1971, vol. 11, pp. 1181-83.

22. R. Petrov, L. Kestens and Y. Houbaert: *Iron Steel Inst. Jpn. Int.*, 2001, vol. 41, pp. 883-90.
23. D. Quidort and Y.J.M. Brechet: *Iron Steel Inst. Jpn. Int.*, 2002, vol. 42, pp. 1010-17.
24. K. Mukunthan and E.B. Hawbolt: *Metall. Trans. A.*, 1996, vol. 27A, pp. 3410-23.
25. K.J. Lee: *Scripta Mater.*, 1999, vol. 40, pp. 837-43.
26. R.A. Oriani: *Acta Metall.*, 1964, vol. 12, pp. 1399-409.
27. H. Hu and S.R. Goodman: *Metall. Trans.*, 1970, vol. 1, pp. 3057-64.
28. W.C. Leslie, F.J. Plecity, and J.T. Michalak: *Trans. TMS-AIME*, 1961, vol. 221, pp. 691-700.
29. W.C. Leslie, F.J. Plecity, and F.W. Aul: *Trans. TMS-AIME*, 1961, vol. 221, pp. 982-89.
30. E.A. Simielli, S. Yue, and J.J. Jonas: *Metall. Trans. A*, 1992, vol. 23A, pp. 597-608.
31. G.J. Shiflet and H.I. Aaronson: *Metall. Trans. A*, 1990, vol. 21A, pp. 1413-32.
32. K. Magee, K. Mukunthan, and E.B. Hawbolt: in *Recrystallization '90*, T. Chandra, ed., TMS, Warrendale, PA, 1990, pp. 393-98.
33. F.J. Humphreys and M. Hatherly: *Recrystallization and Related Annealing Phenomena*, 1st ed., Pergamon, New York, NY, 1995, pp. 127-71.
34. H. Oikawa: *Technol. Rep. Tohoku Univ.*, 1983, vol. 48, pp. 7-77.
35. J. Huang; R.P. Hammond, K. Conlon, and W.J. Poole: *Proc. Int. Conf. on TRIP-Aided High Strength Ferrous Alloys*, B.C. De Cooman, ed., Wissenschaftsverlag Mainz GmbH, Aachen, 2002, pp. 187-91.
36. Mecozzi, J. Sietsma, S. van der Zwaag, M. Apel, P. Schaffnit, and I. Steinbach: in *Austenite Formation and Decomposition*, E.B. Damm and M.J. Merwin, eds., ISS and TMS, Warrendale, PA, 2003, pp. 353-66.